frontiers | Frontiers in Materials

REVIEW
published: 22 July 2022
doi: 10.3389/fmats.2022.954126

Thermophysical Property Measurements of Refractory Oxide Melts With an Electrostatic Levitation Furnace in the International Space Station

Takehiko Ishikawa[1]*, *Paul-François Paradis*[2] and *Chihiro Koyama*[1]

[1]Japan Aerospace Exploration Agency, Tsukuba, Japan, [2]INO, Quebec City, QC, Canada

Due to their high melting temperatures and the risk of contamination from the crucibles, molten oxides which melting temperatures are above 2000 °C can hardly be processed using conventional methods. This explains that their thermophysical properties are very scarce. Containerless methods with gas flows have been developed and several thermophysical properties such as density, surface tension, and viscosity have been reported. However, the gas flow has detrimental side effects such as deformation of the sample and induction of internal flows in the molten sample, which affect the accuracy of the measurements. The electrostatic levitation furnace onboard the International Space Station (ISS-ELF), which utilizes the Coulomb force to levitate and melt samples in microgravity, has several advantages for thermophysical property measurements of refractory oxide melts. Levitation without a gas flow coupled to a reduced gravity environment minimizes the required levitation (positioning) force and reduces the deformation as well as the internal flow. This report briefly introduces the ISS-ELF facility and the thermophysical property measurement methods. The measured density, surface tension, and viscosity of molten Al_2O_3 are then presented and compared with the ones obtained by other methods. Finally, the measured data of refractory oxides whose melting temperatures are above 2,400 °C are summarized.

Keywords: levitation, high temperature melt, density, surface tension, viscosity

OPEN ACCESS

Edited by:
Stefan Karlsson,
RISE Research Institutes of Sweden, Sweden

Reviewed by:
Way Foong Lim,
Universiti Sains Malaysia (USM), Malaysia
Osama A. Fouad,
Head of Nanostructured Materials and Nanotechnology Department, Egypt

***Correspondence:**
Takehiko Ishikawa
ishikawa.takehiko@jaxa.jp

Specialty section:
This article was submitted to Ceramics and Glass, a section of the journal Frontiers in Materials

Received: *27 May 2022*
Accepted: *24 June 2022*
Published: *22 July 2022*

Citation:
Ishikawa T, Paradis P-F and Koyama C (2022) Thermophysical Property Measurements of Refractory Oxide Melts With an Electrostatic Levitation Furnace in the International Space Station. Front. Mater. 9:954126. doi: 10.3389/fmats.2022.954126

1 INTRODUCTION

As additive manufacturing (3D printing) techniques are progressing with ceramics materials (Chen et al., 2019), demands for thermophysical properties of oxide melts are increasing (Ushakov et al., 2021). However, due to their high melting temperatures and the risk linked with contamination from walls, the thermophysical property measurements of molten oxides are difficult with conventional techniques using crucibles. Except for UO_2 (Tsai and Olander, 1972; Woodley, 1974; Fink, 2000), thermophysical properties such as density, surface tension, and viscosity are rarely obtained. Levitation methods circumvent the above-mentioned problems associated with crucibles and enable the handling of refractory oxide melts. The electromagnetic levitation method is widely used for metals and alloys (Brillo and Egry, 2003). However, it is only applicable for conductors and cannot be used for oxide samples. So far, the levitation methods using gas flows are utilized to levitate oxide melts.

Aerodynamic levitation is the simplest among the levitation methods. It uses a conical nozzle through which a gas flows and creates a stable point (pressure minimum) where a sample can be stably levitated (Oran and Berge, 1982, Nordine and Atkins, 1982, and Paradis et al., 1996). Combined with high power lasers, the levitated sample can be heated and melted. Typically, the sample size is between 1 and 3 mm in diameter and the shape of a molten sample is nearly spherical. Steady sample levitation can be achieved by controlling the gas flow rate. Visibility of the sample is poorer than other methods since the lower part of the sample is always covered by the nozzle. Moreover, the lower hemisphere of the sample is cooled by the gas flow, which creates a temperature gradient in the sample. This temperature gradient can be minimized by adding another laser beam heating from the bottom. Sample rotation may be introduced by a misalignment of the heating lasers or by a slight slant of the nozzle (Arai et al., 2003). Density, surface tension, and viscosity of molten oxides have been reported using this approach.

Because of its simplicity, ADLs have been combined with other instruments such as X-ray diffraction facilities (Landron et al., 1999). The splitable nozzle innovated by Arai et al. (Arai et al., 2003) has been used both in a drop carolimetry device (Ushakov et al., 2017) and novel surface tension methods using droplet impingement and bounce (Kondo et al., 2020; Sun et al., 2021a).

In the gas film levitation method (GFL), the positioning of a molten sample is performed on a thin gas-film, formed between the sample and a pressurized porous diffuser. Relatively large samples (up to 10 g of Cu, Ag, and Au) can be handled with this method. The bottom of the sample is hidden by a diffuser. The shape of the molten sample is usually flat, like that of sessile drop due to gravitational sagging. To heat the sample, the levitator is inserted in a furnace or combined with an electromagnetic heating system, which limits the maximum operation temperature. Due to the short distance (<100 μm) between the levitated sample and the lower diffuser, experiments are very difficult. Incorrect experimental settings can result in undesirable contacts between the droplet and the graphite diffuser and consequently in the failure of levitation. This technique was used for research on oxides and metallic glass-forming melts (Barbé et al., 1999; Piluso et al., 2002). Later, the technique was used to measure the thermophysical properties of the ZrO_2-Al_2O_3 system over the 1700–2,350°C temperature interval (Grishchenko and Piluso, 2011).

The aero-acoustic levitation (AAL) method levitates a sample with a gas jet and stabilizes it by acoustic forces using surrounding transducers (Weber et al., 1994; Nordine et al., 2012). The sample position is monitored, and the acoustic forces are adjusted using a feedback control algorithm. The typical sample size is around 1–3 mm in diameter. The shape of the levitated melts, determined by surface tension and gravitational forces, is generally oblate spheroid. The sample is sometimes slightly asymmetric and experiences a slight precession. Density can nonetheless be obtained from the image analysis of the sample with the assumption that it is axisymmetric (Ushakov et al., 2021). Measurement techniques for other thermophysical properties (surface tension, viscosity) have not been reported so far.

All above mentioned methods have disadvantages due to the gas flow. Deformation of the sample shape from that of a sphere reduces the accuracy on image-based volume calculation. Moreover, the gas flow induces a flow inside of the molten sample due to gas shearing forces in addition to thermal gradients. Although the effects of internal flow on viscosity measurements have been observed on the electromagnetically levitated samples in microgravity, its effects on viscosity in ADL experiments have not been examined.

The electrostatic levitation method (ESL) utilizes Coulomb force between a charged sample and surrounding electrodes to levitate a sample against gravity. High speed feedback control is necessary to stably levitate a sample, and, therefore, complicated instrumentation is needed (Rhim et al., 1985; Rhim et al., 1993). The typical sample size is 1–3 mm in diameter and full view of the sample is available. The levitated sample is heated by high power lasers.

Since it is not subject to a gas flow, a levitated molten sample is almost spherical (slightly prolate due to gravity). The internal flow mainly attributable due to natural convection is small and its effect on viscosity is negligible. The ESL method is widely used for metals and alloys with high vacuum environments on Earth. Density (Chung et al., 1996), surface tension, viscosity (Rhim et al., 1999), and heat capacity (Rulison and Rhim, 1994) have been reported on variety of metals/alloys (Ishikawa et al., 2011; Paradis et al., 2013).

In principle, any sample can be handled as far as it has enough charges on its surface. However, the levitation of oxide samples with ESL on the ground is very challenging due to the reasons stated below. To levitate a sample against gravity, a certain amount of surface charge (around 10^{-10} C) and a huge electric field (10–20 kV/cm) are needed. These requirements can be easily satisfied for conductive samples (metals/alloys) under high vacuum environment. However, it is very difficult to accumulate enough electrical charges on oxide samples. Moreover, the oxide samples need to be processed under gaseous environment to prevent evaporation, where a huge electric field cannot be applied because electric discharges between electrodes occurs easily. For these reasons, only a few samples (namely $BaTiO_3$, $Y_3Al_5O_{12}$, Nd-$CaAl_2O_{15}$, Al_2O_3, and $BiFeO_3$) have been reported to be successfully levitated and melted in ground-based ESL experiments.

In microgravity, a large electric field is not necessary, and restrictions are drastically relieved, allowing to handle oxide samples with much fewer electrical charges. Levitation experiments can be conducted in gaseous environment without worrying about electric discharges between electrodes. Moreover, the molten sample becomes perfectly spherical and internal natural convection is suppressed. Microgravity is therefore a very favorable environment for the thermophysical property measurements of high temperature oxide melts with ESL.

The electrostatic levitation furnace onboard the ISS (ISS-ELF) has been developed by the Japan Aerospace Exploration Agency (JAXA) and has been operational since 2016. To validate and demonstrate the capability of thermophysical property measurements of molten oxides at extremely high

FIGURE 1 | Images of a molten Al_2O_3 sample levitated in the ISS-ELF: **(A)** Overview with surrounding 6 electrodes; **(B)** Image taken by a built-in camera in the pyrometer; **(C)** A magnified image of a UV backlit sample.

temperatures, molten lanthanoid sesquioxides (Ln_2O_3, where Ln = La, Ce, Pr, Nd, Sm, Eu, Gd, Tb, Dy, Ho, Er, Tm, Yb, Lu), ZrO_2 and HfO_2 have been selected as main targets of the project.

This paper briefly describes the facility as well as the measurement methods and reports the obtained thermophysical properties. The effect of container walls and important tips for volume measurements are discussed by comparing the measured properties of molten Al_2O_3.

2 METHODS

2.1 ISS-ELF

Detailed descriptions of the facility are found in earlier publications, but are briefly summarized here for completeness (Ishikawa et al., 2018; Tamaru et al., 2018). A positively charged sample can be levitated among three pairs of electrodes orthogonally located against each other (**Figure 1A**). A collimated laser beam (around 20 mm in diameter) from a diode laser emitting at a wavelength of 660 nm projects a shadow of the sample on a position sensor where vertical and horizontal sample positions are measured. Two sets of the projection laser and position sensor are orthogonally placed to measure the tridimensional sample position. The position signals are sent to a controller where the position control voltages are calculated using a PD (Proportional- Differential) control algorithm.

The sample is heated by four semiconductor lasers (980 nm, 40 W power each). To maintain a good temperature homogeneity of the sample, these lasers are arranged in a tetrahedral heating geometry around the sample. Each laser power can be controlled by commands from the ground. Laser beams are focused on a ~0.5 mm diameter spot at the sample position. The sample temperature is measured by a commercial pyrometer (IMPAC IGA140) through sapphire windows. The pyrometer measures the radiation intensity (1.45–1.8 μm in wavelength) from the sample. Since the emissivity setting on the pyrometer cannot be changed from the ground command, it remains at 1.0. The measurement temperature range is from 300°C to 3,000°C and the data acquisition occurs with a 100 Hz frequency. The actual sample temperature can be determined using the temperature plateau after recalescence and the known melting temperature of the sample. The pyrometer also contains a built-in video camera with which it can be easily confirmed that the sample stays in the measuring spot of the pyrometer (**Figure 1B**).

The other camera (a black and white camera with a non-telecentric zoom lens) gives a magnified image of a UV backlit sample (**Figure 1C**). Using the video images (taken with a 60 Hz frequency interval) from this camera, the density of the sample can be calculated. Other than the exchanges of sample holders by the crew members, all operations of the ISS-ELF are remotely conducted from the ground. Experiments were conducted under a dry air pressurized atmosphere (2×10^5 Pa).

2.2 Thermophysical Property Measurements

2.2.1 Density

Density (ρ) can be calculated by dividing the sample mass (m) by its volume (V). Therefore, the measurements of density are done by volume measurements. The volumes of levitated melts are obtained from sample images with the assumption that the molten samples are axisymmetric. To achieve this, the sample images shall be taken from an angle perpendicular to the axis. Usually, the axis is vertical, and the cameras are in the horizontal plane.

In the earlier versions of ADL, the conical nozzle was very deep, and the sample was surrounded by the nozzle and hidden from the sides. Sample images were taken from the top, parallel to the axis, which resulted in erroneous volume measurement. In recent measurements, shallow nozzles are employed which allowed improved, although not total, side views of the sample.

The perimeter of the sample is determined by computer-based image analyses which require a good contrast between the sample and the background. At high temperature, the sample irradiance is very large in the infrared portion of the spectrum, which blurs the sample contour and causes overestimation of the sample volume. This can be avoided by taking images in the 380 (Ultra-Violet) to 530 nm (green) wavelength range, where the sample irradiance is less pronounced. This setup can be easily applied using a proper back light and adding an optical bandpass filter in front of the camera (Ishikawa et al., 2001).

In our measurements with the ISS-ELF, 400 edge points are detected and converted to polar coordinates (R,θ). Then, these

points are fit with the spherical harmonic functions through sixth order as

$$R(\theta) = \sum_{n=0}^{6} c_n P_n(\cos\theta) \tag{1}$$

Where $P_n(\cos\theta)$ are the nth order Legendre polynomials and c_n are the coefficients which are determined to minimize the following value

$$F = \sum_{j=1}^{400} \left\{ R_j - R_j(\theta) \right\}^2 \tag{2}$$

Then, the volume is calculated by the following equation

$$V = \frac{2\pi}{3} \int_0^{\pi} R^3(\theta) \sin\theta d\theta \tag{3}$$

Similar treatments are executed with the ADL, AAL, and GFL methods for volume calculations.

2.2.2 Surface Tension and Viscosity

Surface tensions and viscosities of molten samples are obtained by the drop oscillation method for ADL and ESL. Detailed measurement procedures are described by Rhim et al. (Rhim et al., 1999) for ESL and by Langstaff et al. (Langstaff et al., 2013) for ADL. An isolated liquid drop (free from external force) assumes a spherical shape due to the uniform surface tension. If the drop undergoes a small amplitude axisymmetric oscillation, the drop shape $r(t)$, in the weak damping limit, can be described by (Rayleigh, 1879)

$$r(t) = r_0 + \sum_{n=2}^{\infty} r_n \cos(\omega_n t) \mathrm{P}_n(\cos\theta) \exp\left(\frac{-t}{\tau_n}\right) \tag{4}$$

Where r_0 is the radius of the drop when it assumes a spherical shape, θ is the angle measured between the vertical axis and the radial direction, and r_n is the oscillation amplitude of the nth mode. The characteristic oscillation frequency ω_n corresponding to the nth mode is given by

$$\omega_n^2 = n(n-1)(n+2)\frac{\gamma}{\rho r_0^3} \tag{5}$$

Where γ is the surface tension of the sample. The damping constant τ_n is given by (Lamb, 1932).

$$\frac{1}{\tau_n} = (n-1)(2n+1)\frac{\eta}{\rho r_0^2} \tag{6}$$

Where η is the viscosity of the sample.

With the mode 2 oscillation, the surface tension and viscosity of the sample can be obtained by

$$\gamma = \frac{\rho r_0^3 \omega_2^2}{8}, \text{and} \tag{7}$$

$$\eta = \frac{\rho r_0^2}{5\tau_2}. \tag{8}$$

In the case of ESL, a forced oscillation on the molten sample is achieved by superimposing a sinusoidal excitation voltage on the levitation electric field. When the frequency of the sinusoidal input matches the characteristic oscillation frequency (ω_2), the sample exhibits a large deformation due to resonance (Rhim et al., 1999).

A forced oscillation in ADL is done by pulsing a gas stream by a pair of loudspeakers inserted in the gas line (Langstaff et al., 2013). A mode 2 oscillation with a large amplitude can be obtained by dropping and bouncing the sample on a platform (Sun et al., 2021a).

Measurement of the sample oscillation is done by two methods. In the first method, a high-speed camera is used to record the images which are analyzed to obtain the horizontal/vertical diameters of the sample. By analyzing the fluctuation of the diameters as a function of time, ω_2 and τ_2 can be obtained. This method can visually confirm that mode 2 oscillation is excited. However, it requires to analyze more than 100 still images to get a time-sample deformation profile and this is very time consuming. In another method, a collimated laser beam projects a sample shadow on the power meter covered with a slit (Rhim et al., 1999). The sample deformation is then detected as a fluctuation of the diode laser power onto the power meter. This method is rather simple and can quickly help estimate ω_2 and τ_2. However, the oscillation mode cannot be ensured. The ISS-ELF employs the second method because of its simplicity. In that case, a collimated laser beam used for sample position sensing is divided by a beam splitter and the sample shadow is projected onto a power meter. The sinusoidal voltages which excite an oscillatory sample deformation are superimposed to an electrode (**Figure 2A**). The sample deformation is detected as a fluctuation of the diode laser power by the power meter. When the excitation voltage is terminated, the sample oscillation gradually stops due to its viscosity. The signal from the power meter is captured for 5 s with a 5,000 Hz time resolution. A typical oscillation signal is shown in **Figure 2B**.

Surface tension can also be determined from the stable sample shape in GFL, like the sessile drop method. GFL has also the capability to measure viscosity with two different modes, periodic and aperiodic. The measurement in the periodic mode is similar to that of the oscillation drop method for ADL and ESL and is used for low viscosity melts. The GFL can make a large shape deformation on the highly viscous materials (over 1 Pa·s) to measure the viscosity with the aperiodic mode.

A new technique, namely the drop impingement method, was recently reported to measure surface tension (Kondo et al., 2020). In this technique, an aerodynamically levitated sample is dropped from a splitable nozzle and impinges on a plate. The change of the surface energy during impingement is calculated and the surface tension is evaluated.

3 RESULTS AND DISCUSSION

3.1 Thermophysical Properties of Al_2O_3 Melts

The validation of the thermophysical property measurement capability of the ISS-ELF was conducted using Al_2O_3 melts, because a relatively large number of reference values taken

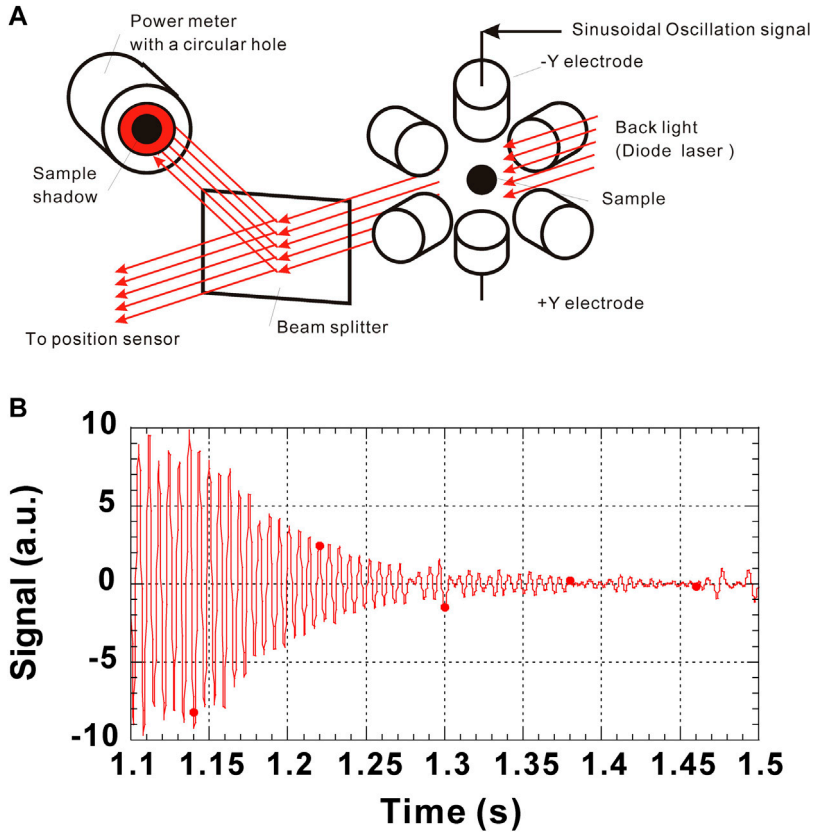

FIGURE 2 | Drop oscillation system of the ISS-ELF: **(A)** Schematic drawing of how to excite and observe drop oscillations; **(B)** A typical oscillation signal obtained by the power meter.

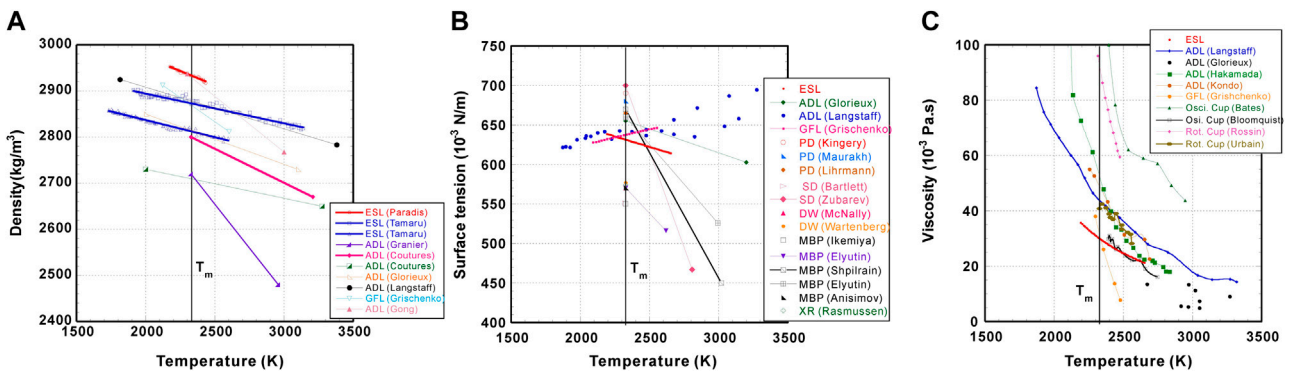

FIGURE 3 | Measured thermophysical properties of molten Al_2O_3 vs. temperature: **(A)** Density; **(B)** Surface tension; **(C)** Viscosity. The correlation coefficient (R) of our measurements (ESL) is 0.98 for density, 0.43 for surface tension, and 0.61 for viscosity, respectively.

by both conventional and containerless methods were available.

3.1.1 Density

The density values of molten Al_2O_3 measured with the ISS-ELF and their temperature dependence as well as data found in literature are shown in **Figure 3A** and **Table 1**. It is clearly seen that the density measured at the melting temperature (ρ_m) by containerless methods (ESL, ADL, and GFL) agrees well, ranging from 2.71 to 2.93 g/cm^3, indicating a divergence of ±3.9%. Since earlier measurements with ADLs (Granier and Heurtault, 1983; Coutures and Rand, 1989; Glorieux et al., 1999) employed non-optimal video settings (viewing

TABLE 1 | Density of molten Al_2O_3.

ρ_m (10^3 kg m^{-3})	dρ/dT (kg·m^{-3}·K^{-1})	Temperature (K)	Reference
2.93	−0.12	2,175–2,435	ESL (Paradis et al., 2004)
2.87	−0.064	1913–3,139	ESL (Tamaru et al., 2018)
2.81	−0.074	1732–2,597	ESL (Tamaru et al., 2018)
2.9	−0.09	1900–3,240	ADL (Langstaff et al., 2013)
2.93	−0.242	2,300–3,000	ADL (Gong et al., 2022)
2.79	−0.117	2000–3,100	ADL (Glorieux et al., 1999)
2.71	−0.0678	2000–3,275	ADL (Coutures et al., 1994)
2.80	−0.151	2,327–3,210	ADL (Coutures et al., 1994)
2.72	−0.28	2,323–2,965	ADL (Granier and Heurtault, 1983)
2.87	−0.2098	2,123–2,603	GFL (Grishchenko and Piluso, 2011)
2.69	−0.79	2,320–3,100	SD (Zubarev et al., 1969)
2.55		2,327	PD (Wartenberg et al., 1936)
3.05		2,327	PD (Kozakevitch, 1960)
2.97		2,327	PD (Kingery, 1959)
3.06		2,327	MBP (Ikemiya et al., 1993)
3.06	−0.965	2,323–3,023	MBP (Shpil'rain et al., 1973)
2.98	−1.15	2,325–2,775	MBP (Elyutin et al., 1973)
3.04	−1.15	2,323–2,828	Archimedean (Mitin and Nagibin, 1970)
3.05	−1.127	2,375–2,625	Archimedean (Kirshenbaum and Cahill, 1960)
3.03	−0.752	2,323–2,673	X-radiograph (XR) (Rasmussen and Nelson, 1971)

SD: sessile drop, PD: pendant drop.

TABLE 2 | Surface tension of molten Al_2O_3.

γ_m (10^{-3}N·m^{-1})	dg/dT (10^{-3}N·m^{-1}·K^{-1})	Temperature (K)	Reference
632	-5.3×10^{-2}	2,193–2,653	ESL (Paradis and Ishikawa, 2005; Ishikawa et al., 2022a)
650	-3.9×10^{-2}	2,327–3,200	ADL (Glorieux et al., 2001)
~640	(3.5×10^{-2})	1870–3,275	ADL (Langstaff et al., 2013)
638	[a]	2,123–2,603	GFL (Grishchenko and Piluso, 2011)
690	—	2,327	PD (Kingery, 1959)
680	—	2,327	PD (Maurakh et al., 1967)
665	—	2,327	PD (Lihrmann and Haggerty, 1985)
551	—	2,327	SD (Bartlett and Hall, 1965)
700	-4.8×10^{-1}	2,327–2,810	SD (Zubarev et al., 1969)
570	—	2,327	DW (McNally et al., 1968)
577	—	2,327	DW (Wartenberg et al., 1936)
550	—	2,327	MBP (Ikemiya et al., 1993)
570	-1.8×10^{-1}	2,327–2,620	MBP (ElyutinMitin and Nagibin, 1971)
670	-3.2×10^{-1}	2,327–3,020	MBP (Shpil'rain et al., 1973)
660	-2.0×10^{-1}	2,327–2,995	MBP (Elyutin et al., 1973)
570	—	2,327	MBP (Anisimov et al., 1977)
574	—	2,327	X-radiograph (XR) (Rasmussen and Nelson, 1971)

[a]*DW: drop weight, MBP: maximum bubble pressure.*
$\gamma(T) = 517.286 + 7.658 \times 10^{-2}T - 8.7 \times 10^{-6}T^2$.

from top and no back light), their density values were underestimated. By omitting these values, the divergence is reduced to ±2.1%, which is within the experimental uncertainty. Even though a part of the sample is hidden in ADL setups, the introduced error on the volume estimation is very small.

The values of ρ_m measured by conventional methods exhibited more scatter, ranging from 2.69 to 3.06 (±6.4%). Moreover, the measured temperature coefficients (dρ/dT) showed large differences between conventional and containerless techniques. While absolute values of dρ/dTs obtained by containerless methods are less than 0.3, those reported by conventional methods are more than 0.8. Contamination from the crucibles may cause this discrepancy.

Recently, Gong et al. (Gong et al., 2022) reported the density of Al_2O_3 with ADL. The sample image was taken from the side without proper backlighting, which leaded to blurred images and resulted in a relatively large temperature coefficient.

3.1.2 Surface Tension

The surface tension values of molten Al_2O_3 taken by the ISS-ELF and their temperature dependence as well as the ones found in the literature are depicted in **Figure 3B** and listed in **Table 2**. Note that the surface tension data obtained by the ground-based ESL and the ISS-ELF showed good agreement (Ishikawa et al., 2022a). The combined data are shown in the **Table 2** and **Figure 3B**.

TABLE 3 | Viscosity of molten Al_2O_3 at its melting temperature.

η_m (10^{-3} Pa s)	Reference
30	ESL (Paradis and Ishikawa, 2005; Ishikawa et al., 2022a)
45	ADL (Langstaff et al., 2013)
54	ADL (Hakamada et al., 2017)
50	ADL (Kondo et al., 2019)
32	GFL (Grishchenko and Piluso, 2011)
135	Oscillating cup (Bates et al., 1971)
35	Oscillating cup (Bloomquist et al., 1978)
~95	Rotating cup (Rossin, 1964)
42	Rotating cup (Urbain, 1982)

For the surface tension measured at the melting temperature (γ_m), all data obtained containerlessly (ESL and ADL) agree well within their experimental uncertainties, whereas those obtained by conventional methods show wider discrepancies.

In earlier ADL experiments (Glorieux et al., 2001), there was no technique to add an external oscillation force. Langstaff et al. came up with an innovative set up to apply an external force (Langstaff et al., 2013). However, this external oscillation force could have possibly excited non-axisymmetric mode-2 oscillations which resulted in odd (positive) temperature dependence. The temperature dependence obtained by GFL also shows positive temperature dependence (Grishchenko and Piluso, 2011).

Except for the pendant drop method (PD), γ_m values measured by conventional methods display scatter and show huge temperature dependences, indicating that the reaction between the samples and the container affected the surface tension. Since crucibles were not used in PD, the measured values agree well among all data taken with this technique. Their γ_ms are slightly higher than the ones obtained by ESL and ADL, maybe because of the difference in the density values used for calculation.

3.1.3 Viscosity

The viscosity of molten Al_2O_3 and its temperature dependence found in the literature are listed in **Table 3** as well as depicted in **Figure 3C**. The viscosity data obtained by the ground-based ESL and the ISS-ELF (Ishikawa et al., 2022a) are combined and are also listed in **Table 3** and **Figure 3C**.

Like those of density and surface tension, the values of viscosity measured at the melting temperature (η_m) by containerless methods (ESL, GFL and ADL) show better agreement than those obtained by conventional methods. However, the values measured by ADLs are more than 50% higher than those reported by ESL, which is more than the experimental uncertainty (30%). It has been reported that the viscosity values measured with an electromagnetic levitation furnace increased up to 2 to 8 times due to the internal flow (Xiao et al., 2021). As for ADL experiments, the gas flow around the sample could potentially cause flow inside the sample which may impact the viscosity measurements.

3.2 Thermophysical Properties of Lanthanoid Sesquioxides, ZrO_2, and HfO_2

Melting temperatures of lanthanoid sesquioxides (Coutures and Rand, 1989), ZrO_2, and HfO_2 are more than 2,400°C, which is more than 250 K higher than that of Al_2O_3. Therefore, it is very difficult to melt these specimens with conventional techniques explaining why literature values are very rare. Most of the data have been measured by containerless methods. The thermophysical properties of Ln_2O_3, where Ln = Gd, Tb, Ho, Er, Tm, Yb, and Lu, have been measured in the ISS-ELF. For Ln = La, Ce, Pr, Nd, Sm, Eu, and Dy, experiments were postponed due to a technical issue encountered with sample preservation during the long-term storage before and after the microgravity experiments in the ISS. These samples easily absorb moisture and naturally break into powders.

3.2.1 Density

The density data are listed in **Table 4**, highlighting those of lanthanoid sesquioxides (Koyama et al., 2021; Ishikawa et al., 2022b) that have been systematically measured using the ISS-ELF (**Figure 4A**).

As shown in **Figure 4B**, it was found that the molar volumes of lanthanoid sesquioxides as well as those of Ga_2O_3 (Dingwell, 1992) and Al_2O_3 show strong relations with their ionic radii. Data taken by AAL (Ushakov et al., 2021) agree well with the values measured with the ISS-ELF. The density data taken by Granier et al. using ADL (Granier and Heurtault, 1998) are around 7% lower, most likely because improper camera settings leaded to the overestimation of the sample volume.

Levitated ZrO_2 and HfO_2 samples have not been successfully melted in the ISS-ELF yet, mainly due to the unstable surface charge encountered during heating. We are confident that optimization of the position control parameters will solve this problem. Two density data sets have been taken for ZrO_2 by ADLs (Kohara et al., 2014; Kondo et al., 2019) and those agree well within the experimental uncertainty. Only one density data set, measured by AAL, has been reported for HfO_2 (Ushakov et al., 2021).

3.2.2 Surface Tension and Viscosity

The measured surface tension and viscosity data are listed in **Table 5** and **Table 6**, respectively. For both surface tension and viscosity, the measured data are scarcer than those of density. This is attributable to the fact that the oscillation drop experiments in ISS-ELF are much harder to perform than those required for density measurements since more accurate sample position control is required. So far, the surface tension and viscosity of Tb_2O_3 were measured with the ISS-ELF. The measured surface tension and viscosity of Tb_2O_3 as a function of temperature are respectively shown in **Figures 5A,B** (Ishikawa et al., 2022a). The surface tension of ZrO_2 measured by the drop impingement method as well as by the drop oscillation method with ADL were reported (Kondo et al., 2020). In addition, the viscosity of ZrO_2 was measured by the drop oscillation method combined with ADL (Kondo et al., 2019).

TABLE 4 | Density of molten Ln_2O_3, ZrO_2, and HfO_2.

Samples	T_m (K)	ρ_m (kg·m^{-3})	dρ/dT (kg·m^{-3}·K^{-1})	Remarks
Y_2O_3	2,704	4,600 ± 150		AAL (Ushakov et al., 2021)
		4,420	−0.8927 ± 0.222	ADL (Granier and Heurtault, 1998)
Gd_2O_3	2,693	7,268 ± 205		ESL (Koyama et al., 2021)
		6,947 ± 340	−1.048 ± 0.112	ADL (Granier and Heurtault, 1998)
Tb_2O_3	2,683	7,451 ± 112		ESL (Koyama et al., 2021)
Ho_2O_3	2,685	8,035 ± 108		ESL (Koyama et al., 2021)
Er_2O_3	2,686	8,170 ± 245		ESL (Koyama et al., 2021)
		7,573 ± 530	−0.3273 ± 0.179	ADL (Granier and Heurtault, 1998)
Tm_2O_3	2,698	8,304 ± 148	−0.18 ± 0.05	ESL (Ishikawa et al., 2022b)
Yb_2O_3	2,708	8,425 ± 217	−0.55 ± 0.08	ESL (Ishikawa et al., 2022b)
	2,708	7,940	−0.74 ± 0.13	ADL (Granier and Heurtault, 1998)
	2,708	8,400 ± 200		AAL (Ushakov et al., 2021)
Lu_2O_3	2,763	8,627 ± 240	−0.43 ± 0.08	ESL (Ishikawa et al., 2022b)
ZrO_2	2,983	5,048	−0.89	ADL (Kohara et al., 2014)
		4,690		ADL (Kondo et al., 2019)
HfO_2	3,073	8,200 ± 300		AAL (Ushakov et al., 2021)

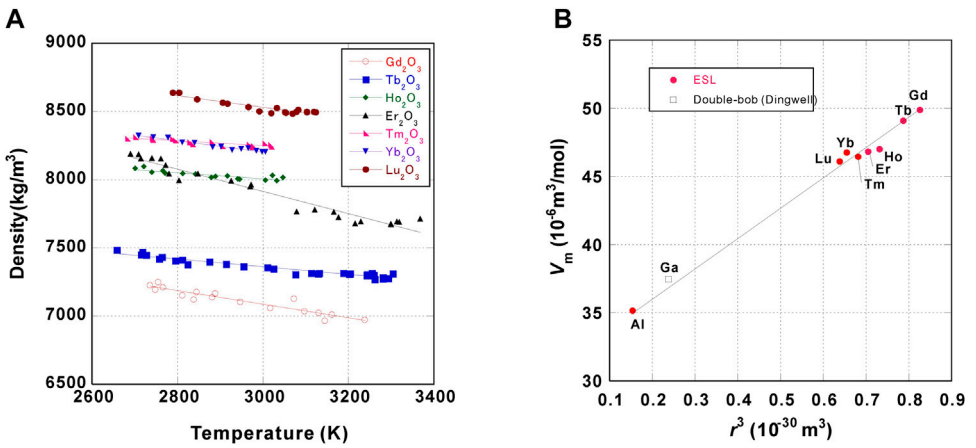

FIGURE 4 | (A) Density of molten lanthanoid sesquioxides as a function of temperature measured by the ISS-ELF. The correlation coefficient (R) for each measurement is 0.94 for Gd_2O_3, 0.96 for Tb_2O_3, 0.87 for Ho_2O_3, 0.97 for Er_2O_3, 0.86 for Tm_2O_3, 0.98 for Yb_2O_3, and 0.94 for Lu_2O_3, respectively; **(B)** Relation between molar volumes of M_2O_3 type oxides at their melting temperatures and their ionic radii.

TABLE 5 | Surface tension of molten Ln_2O_3 and ZrO_2.

Samples	T_m (K)	γ_m (10^{-3} N m^{-1})	dγ/dT (10^{-3} N m^{-1}·K^{-1})	Remarks
Tb_2O_3	2,683	733.4	−0.039	ESL (Ishikawa et al., 2022a)
ZrO_2	2,988	910 ± 10	−0.133 ± 0.116	ADL (Kondo et al., 2020)

TABLE 6 | Viscosity of molten Ln_2O_3 and ZrO_2.

Samples	T_m (K)	η_m (10^{-3}Pa s)	Temperature dependence[a]		Remarks
			η_0 (10^{-3}Pa s)	E (10^3J/mol)	
Tb_2O_3	2,683	26.3	0.33	97.6	ESL (Ishikawa et al., 2022a)
ZrO_2	2,988	13	0.96 ± 0.69	64 ± 20	ADL (Kondo et al., 2019)

[a] η $(T) = \eta_0 exp$ (E/RT), *where R is the gas constant (8.31 J·mol·K^{-1}).*

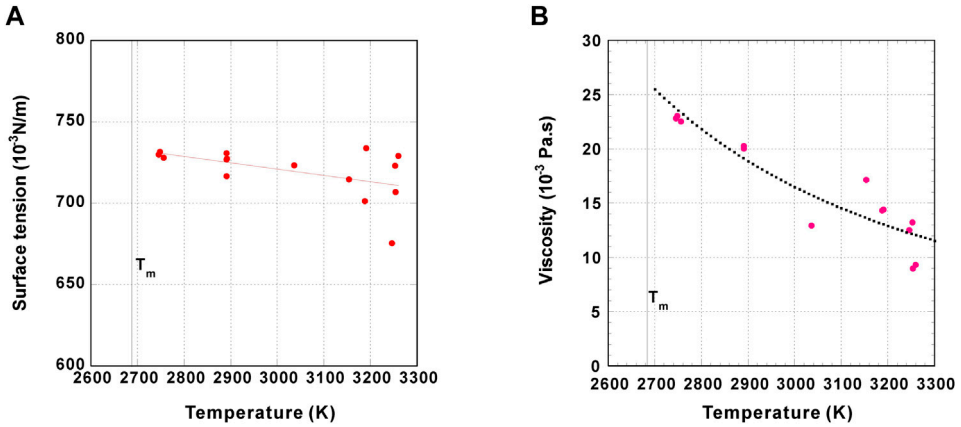

FIGURE 5 | Measured surface tension **(A)** and viscosity **(B)** of molten Tb_2O_3 as a function of temperature. The correlation coefficient (R) of measurement is 0.82 for surface tension and 0.90 for viscosity, respectively.

The viscosity measurements carried out by the drop oscillation method is suitable for viscosity ranging from around 1–30 mPa·s. When the viscosity becomes higher, the oscillation damps too quickly to allow accurate measurements of τ_2, thus introducing a large uncertainty. Moreover, when the viscosity excesses 1 Pa·s, this technique is not applicable either because a periodic deformation does not occur. On the other hand, the viscosity measurements over wide viscosity ranges (1 m Pa·s to over 10 Pa·s) are required for oxide glass research. Like that implemented with GFL, the development of a viscosity measurement method with aperiodic mode is desired for ADL and ESL.

3.2.3 Other Thermophysical Properties

A splitable ADL has been combined with a drop calorimetry system to allow the measurements of the enthalpy of the levitated sample (Ushakov et al., 2017). The heat of fusion of several refractory oxides including Al_2O_3, Yb_2O_3, Lu_2O_3, ZrO_2, and HfO_2 was reported (Ushakov et al., 2018). This experimental set up also has the potential to measure the constant pressure heat capacity.

Heat dissipation from the levitated sample is governed by the following equation.

$$mC_p\frac{dT}{dt} = -\varepsilon_T\sigma_{SB}A\left(T^4 - T_w^4\right) - \kappa A\left(T - T_w\right) + Q \qquad (9)$$

Where, T_w is the temperature of the surrounding wall, ε_T is the total hemispherical emissivity of the sample, σ_{SB} is the Stefan-Boltzmann constant, κ is the overall heat transfer coefficient, A is the sample surface area, and Q is the laser power input. On the right-hand side of **Equation 9**, the first term is the contribution of radiation, and the second term is the contribution of thermal conduction and convection. In the experiments under high vacuum, the second term is negligible and the ratio of the constant pressure heat capacity C_p and ε_T can be calculated using the time-temperature profile during rapid cooling (Q = 0) (Rulison and Rhim, 1994). However, the equation is too complicated to quantitatively calculate C_p in gaseous environment where natural convection exists.

Sun et al. (Sun et al., 2021b) calculated the second term (convective heat loss) in ADL using Ranz-Marshall's equation (Ranz and Marshall, 1952) which is applicable in the case of a steady gas flow. Moreover, using two different inert gases (with different thermal conductivity values) for levitation experiments, C_p values were calculated without knowing ε_Ts. This method has been evaluated with refractory metals. Even though more work is necessary to improve the accuracy of the measurement, this technique can be used for the C_p measurements of refractory oxide melts with ADL.

Natural convection is suppressed in microgravity, and the second term is simply defined as the thermal conduction by the surrounding gas. Therefore, there is a possibility that C_p can be calculated using the time-temperature profile in the ISS-ELF.

AUTHOR CONTRIBUTIONS

Conceptualization by TI and P-FP. Experiments by TI and CK. Validation by P-FP. Original draft preparation by TI. Writing-review and editing by P-FP and CK.

FUNDING

This research is fully supported by Japan Aerospace Exploration Agency. This research is supported by JSPS KEKENHI (Grant No. 20H05882 and 20H05878).

ACKNOWLEDGMENTS

The authors are grateful to the ISS crew members and the ground operation staff for their support during the onboard experiments.

REFERENCES

Anisimov, Yu. S., Grifts, E. F., and Mitin, B. S. (1977). *Izv. Akad. Nauk. SSSR Neorg. Mat.* 13, 1444.

Arai, Y., Paradis, P. -F., Aoyama, T., Ishikawa, T., and Yoda, S. (2003). An aerodynamic levitation system for drop tube and quenching experiments. *Rev. Sci. Instrum.* 74, 1057–1063. doi:10.1063/1.1531826

Barbé, J.-Ch., Parayre, C., Daniel, M., Papoular, M., and Kernevez, N. (1999). High-temperature containerless viscosity measurements by gas-film levitation. *Int. J. Thermophys.* 20, 1071–1083. doi:10.1023/A:1022698619162

Bartlett, R. M., and Hall, J. K. (1965). Wetting of several solids by Al_2O_3 and BeO liquids. *Ceram. Bull.* 44, 444.

Bates, J. L., McNeilly, C. E., and Rasmussen, J. J. (1971). "Properties of molten ceramics," in *Ceramics in severe environments, material science research* (New-York: Plenum Press), 11.

Bloomquist, R. A., Fink, J. K., and Leibowitz, L. (1978). Viscosity of molten alumina. *Am. Ceram. Soc. Bull.* 57, 522.

Brillo, J., and Egry, I. (2003). Density determination of liquid copper, nickel, and their alloys. *Int. J. Thermophys.* 24, 1155–1170. doi:10.1023/A:1025021521945

Chen, Z., Li, Z., Li, J., Liu, C., Lao, C., Fu, Y., et al. (2019). 3D printing of ceramics: A review. *J. Eur. Ceram. Soc.* 39, 661–687. doi:10.1016/j.jeurceramsoc.2018.11.013

Chung, S. K., Thiessen, D. B., and Rhim, W.-K. (1996). A noncontact measurement technique for the density and thermal expansion coefficient of solid and liquid materials. *Rev. Sci. Instrum.* 67, 3175–3181. doi:10.1063/1.1147584

Coutures, J.-P., Rifflet, J.-C., Florian, P., and Massiot, D. (1994). A thermal analysis and very high temperature ^{27}Al NMR study of the solidification behavior in contactless conditions of liquid alumina: Effects of the melt temperature and oxygen partial pressure. *Rev. Int. Hautes Temp. Refract.* 29, 123.

Coutures, J. P., and Rand, M. H. (1989). Melting temperatures of refractory oxides: Part II lanthanoid sesquioxides. *Pure Appl. Chem.* 61, 1461–1482. doi:10.1351/pac198961081461

Dingwell, D. B. (1992). Density of Ga_2O_3 liquid. *J. Am. Ceram. Soc.* 75, 1656–1657. doi:10.1111/j.1151-2916.1992.tb04239.x

Elyutin, V. P., Mitin, B. S., and Anisimov, Yu. S. (1973). *Neo. Mat.* 9, 1585.

Elyutin, V. P., Mitin, B. S., and Nagibin, Y. A. (1971). *Zavod. Lab.* 2, 194.

Fink, J. K. (2000). Thermophysical properties of uranium dioxide. *J. Nucl. Mater.* 279, 1–18. doi:10.1016/S0022-3115(99)00273-1

Glorieux, B., Millot, F., Rifflet, J. C., and Coutures, J.-P. (1999). Density of superheated and undercooled liquid alumina by a contactless method. *Int. J. Thermophys.* 20, 1085–1094. doi:10.1023/A:1022650703233

Glorieux, B., Saboungi, M.-L., Millot, F., Enderby, J., and Rifflet, J.-C. (2001). Aerodynamic levitation: An approach to microgravity. *AIP Conf. Proc.* 552, 316. doi:10.1063/1.1357941

Gong, Y., Zhang, L., Yuan, Y., Guo, Q., Ma, W., Huang, S., et al. (2022). Density measurement of molten drop with aerodynamic levitation and laser heating. *Front. Energy Res.* 10, 892406. doi:10.3389/fenrg.2022.892406

Granier, B., and Heurtault, S. (1998). Density of liquid rare-earth sesquioxides. *J. Am. Ceram. Soc.* 71, C466–C468. doi:10.1111/j.1151-2916.1988.tb07551.x

Granier, B., and Heurtault, S. (1983). Method for measurement of density of liquid refractories. Applications to alumina and yttrium oxide. *Rev. Int. Hautes Temp. Refract.* 20, 31.

Grishchenko, D., and Piluso, P. (2011). Recent progress in the gas-film levitation as a method for thermophysical properties measurements: Application to ZrO_2-Al_2O_3 system. *High. Temp.- High. Press* 40, 127.

Hakamada, S., Nakamura, A., Watanabe, M., and Kargl, F. (2017). Surface oscillation phenomena of aerodynamically levitated molten Al_2O_3. *Int. J. Microgravity Sci. Appl.* 34, 340403. doi:10.15011/ijmsa.34.4_340403

Ikemiya, N., Umemoto, J., Hara, S., and Ogino, K. (1993). Surface tension and densities of molten Al_2O_3, Ti_2O_3, V_2O_5 and Nb_2O_5. *ISIJ Int.* 33, 156–165. doi:10.2355/isijinternational.33.156

Ishikawa, T., Koyama, C., Oda, H., Saruwatari, H., and Paradis, P.-F. (2022a). Status of the electrostatic levitation furnace in the ISS - surface tension and viscosity measurements. *Int. J. Microgravity Sci. Appl.* 39, 390101. doi:10.15011/jasma.39.390101

Ishikawa, T., Koyama, C., Oda, H., Shimonishi, R., Ito, T., and Paradis, P.-F. (2022b). Densities of liquid Tm2O3, Yb2O3, and Lu2O3 measured by an electrostatic levitation furnace onboard the International Space Station. *Metals* 12, 1126. doi:10.3390/met12071126

Ishikawa, T., Koyama, C., Tamaru, H., Saruwatari, H., Ohshio, M., and Nakamura, Y. (2018). Status of the electrostatic levitation furnace in the ISS – evaluation of sample position control -. *Int. J. Microgravity Sci. Appl.* 35, 350205. doi:10.15011//jasma.35.350205

Ishikawa, T., Okada, J. T., Paradis, P.-F., and Watanabe, Y. (2011). Thermophysical property measurements of high temperature melts using an electrostatic levitation method. *Jpn. J. Appl. Phys. (2008).* 50, 11RD03. doi:10.1143/jjap.50.11rd03

Ishikawa, T., Paradis, P.-F., and Yoda, S. (2001). New sample levitation initiation and imaging techniques for the processing of refractory metals with an electrostatic levitator furnace. *Rev. Sci. Instrum.* 72, 2490–2495. doi:10.1063/1.1368861

Kingery, W. D. (1959). Surface tension of some liquid oxides and their temperature coefficients. *J. Am. Ceram. Soc.* 42, 6–10. doi:10.1111/j.1151-2916.1959.tb09134.x

Kirshenbaum, A. D., and Cahill, J. A. (1960). The density of liquid aluminium oxide. *J. Inorg. Nucl. Chem.* 14, 283–287. doi:10.1016/0022-1902(60)80272-2

Kohara, S., Akola, J., Patrikeev, L., Ropo, M., Ohara, K., Itou, M., et al. (2014). Atomic and electronic structures of an extremely fragile liquid. *Nat. Commun.* 5, 5892. doi:10.1038/ncomms6892

Kondo, T., Muta, H., Kurosaki, K., Kargl, F., Yamaji, A., Furuya, M., et al. (2019). Density and viscosity of liquid ZrO_2 measured by aerodynamic levitation technique. *Heliyon* 5, e02049. doi:10.1016/j.heliyon.2019.e02049

Kondo, T., Muta, H., and Ohishi, Y. (2020). Droplet impingement method to measure the surface tension of molten zirconium oxide. *J. Nucl. Sci. Technol.* 57, 889–897. doi:10.1080/00223131.2020.1736681

Koyama, C., Ishikawa, T., Oda, H., Saruwatari, H., Ueno, S., Oshio, M., et al. (2021). Densities of liquid lanthanoid sesquioxides measured with the electrostatic levitation furnace in the ISS. *J. Am. Ceram. Soc.* 104, 2913–2918. doi:10.1111/jace.17674

Kozakevitch, P. (1960). Viscosité et éléments structuraux des aluminosilicates fondus: Laitiers CaO-Al_2O_3-SiO_2 entre 1600 et 2100 °C. *Rev. Mater. Paris.* 57, 149–160. doi:10.1051/metal/196057020149

Lamb, H. (1932). *Hydrodynamics*. 6th ed. Cambridge): Cambridge University Press, 473.

Landron, C., Hennet, L., Berthet, P., Coutures, J.-P., and Berar, J.-F. (1999). Aerodynamic levitation studies of ceramics at very high-temperature: XAFS and XRD. *Jpn. J. Appl. Phys. (2008).* 38, 87. doi:10.7567/jjaps.38s1.87

Langstaff, D., Gunn, M., Greaves, G. N., Marsing, A., and Kargl, F. (2013). Aerodynamic levitator furnace for measuring thermophysical properties of refractory liquids. *Rev. Sci. Instrum.* 84, 124901. doi:10.1063/1.4832115

Lihrmann, J. M., and Haggerty, J. S. (1985). Surface tensions of alumina-containing liquids. *J. Am. Ceram. Soc.* 68, 81–85. doi:10.1111/j.1151-2916.1985.tb15269.x

Maurakh, M. A., Mitin, B. S., and Roitberg, M. B. (1967). *Zavod. Lab.* 33, 984.

McNally, R. N., Yeh, H. C., and Balasubramanian, N. (1968). Surface tension measurements of refractory liquids using the modified drop weight method. *J. Mat. Sci.* 3, 136–138. doi:10.1007/BF00585480

Mitin, B., and Nagibin, Y. A. (1970). Density of liquid alumina. *Russ. J. Phys. Chem.* 44, 741.

Nordine, P. C., and Atkins, R. M. (1982). Aerodynamic levitation of laser-heated solids in gas jets. *Rev. Sci. Instrum.* 53, 1456–1464. doi:10.1063/1.1137196

Nordine, P. C., Merkley, D., Sickel, J., Finkelman, S., Telle, R., Kaiser, A., et al. (2012). A levitation instrument for containerless study of molten materials. *Rev. Sci. Instrum.* 83, 125107. doi:10.1063/1.4770125

Oran, W. A., and Berge, L. H. (1982). Containerless melting and solidification of materials with an aerodynamic levitation system. *Rev. Sci. Instrum.* 53, 851–853. doi:10.1063/1.1137067

Paradis, P.-F., Babin, F., and Gagné, J. -M. (1996). Study of the aerodynamic trap for containerless laser materials processing in microgravity. *Rev. Sci. Instrum.* 67, 262–270. doi:10.1063/1.1146581

Paradis, P.-F., Ishikawa, T., Lee, G.-W., Holland-Moritz, D., Brillo, J., Rhim, W.-K., et al. (2013). Materials properties measurements and particle beam interactions studies using electrostatic levitation. *Mater. Sci. Eng. R Rep.* 76, 1–53. doi:10.1016/j.mser.2013.12.001

Paradis, P.-F., Ishikawa, T., Saita, Y., and Yoda, S. (2004). Non-contact thermophysical property measurements of liquid and undercooled alumina. *Jpn. J. Appl. Phys. (2008).* 43, 1496–1500. doi:10.1143/JJAP.43.1496

Paradis, P.-F., and Ishikawa, T. (2005). Surface tension and viscosity measurements of liquid and undercooled alumina by containerless techniques. *Jpn. J. Appl. Phys. (2008).* 44, 5082–5085. doi:10.1143/JJAP.44.5082

Piluso, P., Monerris, J., Journeau, C., and Cognet, G. (2002). Viscosity measurements of ceramic oxides by aerodynamic levitation. *Int. J. Thermophys.* 23, 1229–1240. doi:10.1023/a:1019844304593

Ranz, W. E., and Marshall, W. R., Jr (1952). Evaporation from drops, part I. *Chem. Eng. Prog.* 48, 141.

Rasmussen, J. J., and Nelson, R. P. J. (1971). Surface tension and density of molten $A1_2O_3$. *J. Am. Ceram. Soc.* 54, 398–401. doi:10.1111/j.1151-2916.1971.tb12330.x

Rayleigh, L. (1879). On the capillary phenomena of jets. *Proc. R. Soc. Lond.* 29, 71.

Rhim, W.-K., Chung, S. K., Barber, D., Man, K. F., Gutt, G., Rulison, A., et al. (1993). An electrostatic levitator for high-temperature containerless materials processing in 1-g. *Rev. Sci. Instrum.* 64, 2961–2970. doi:10.1063/1.1144475

Rhim, W.-K., Collender, M., Hyson, M. T., Simms, W. T., and Elleman, D. D. (1985). Development of an electrostatic positioner for space material processing. *Rev. Sci. Instrum.* 56, 307–317. doi:10.1063/1.1138349

Rhim, W.-K., Ohsaka, K., Paradis, P.-F., and Spjut, R. E. (1999). Noncontact technique for measuring surface tension and viscosity of molten materials using high temperature electrostatic levitation. *Rev. Sci. Instrum.* 70, 2796–2801. doi:10.1063/1.1149797

Rossin, R. (1964). Viscosity of liquid slags belonging to the ternary system SiO_2-Al_2O_3-CaO. *Rev. Hautes Temp. Refract.* 1, 159.

Rulison, A. J., and Rhim, W.-K. (1994). A noncontact measurement technique for the specific heat and total hemispherical emissivity of undercooled refractory materials. *Rev. Sci. Instrum.* 65, 695–700. doi:10.1063/1.1145087

Shpil'rain, E. E., Yakimovich, K. A., and Tsitsarkin, A. F. (1973). Experimental study of the density of liquid alumina up to 2750°C. *High. Temp.-High. Press.* 5, 191.

Sun, Y., Muta, H., and Ohishi, Y. (2021b). Multiple-gas cooling method for constant-pressure heat capacity measurement of liquid metals using aerodynamic levitator. *Rev. Sci. Instrum.* 92, 095102. doi:10.1063/5.0055555

Sun, Y., Muta, H., and Ohishi, Y. (2021a). Novel method for surface tension measurement: The drop-bounce method. *Microgravity Sci. Technol.* 33, 32. doi:10.1007/s12217-021-09883-7

Tamaru, H., Koyama, C., Saruwatari, H., Nakamura, Y., Ishikawa, T., Takada, T., et al. (2018). Status of the electrostatic levitation furnace (ELF) in the ISS-KIBO. *Microgravity Sci. Technol.* 30, 643–651. doi:10.1007/s12217-018-9631-8

Tsai, H. C., and Olander, D. R. (1972). The viscosity of molten uranium dioxide. *J. Nucl. Mater.* 44, 83–86. doi:10.1016/0022-3115(72)90132-8

Urbain, G. (1982). Viscosité de l'alumine liquide. *Rev. Int. Hautes Tempér. Réfract.* 19, 55.

Ushakov, S. V., Maram, P. S., Kapush, D., Pavlik, A. J., III, Fyhrie, M., Gallington, L. C., et al. (2018). Phase transformations in oxides above 2000 °C: Experimental technique development. *Adv. Appl. Ceram.* 117, S82–s89. doi:10.1080/17436753.2018.1516267

Ushakov, S. V., Niessen, J., Quirinale, D. G., Prieler, R., Navrotsky, A., Telle, R., et al. (2021). Measurements of density of liquid oxides with an aero-acoustic levitator. *Materials* 14, 822. doi:10.3390/ma14040822

Ushakov, S. V., Shvarev, A., Alexeev, T., Kapush, D., and Novrotsky, A. (2017). Drop-and-catch (DnC) calorimetry using aerodynamic levitation and laser heating. *J. Am. Ceram. Soc.* 100, 754–760. doi:10.1111/jace.14594

Wartenberg, H. V., Wehner, E., and Saran, E. (1936). *Nach. Akad. Wiss. Goettingen* 2, 65.

Weber, J. K. R., Hampton, D. S., Merkley, D. R., Rey, C. A., Zatarski, M. M., Nordine, P. C., et al. (1994). Aero-acoustic levitation: A method for containerless liquid-phase processing at high temperatures. *Rev. Sci. Instrum.* 65, 456–465. doi:10.1063/1.1145157

Woodley, R. E. (1974). The viscosity of molten uranium dioxide. *J. Nucl. Mater.* 50, 103–106. doi:10.1016/0022-3115(74)90066-X

Xiao, X., Brillo, J., Lee, J., Hyers, R. W., and Matson, D. M. (2021). Impact of convection on the damping of an oscillating droplet during viscosity measurement using the ISS-EML facility. *npj Microgravity* 7, 36. doi:10.1038/s41526-021-00166-4

Zubarev, Y. V., Kostikov, V. I., Mitin, B. S., Nagibin, Y. A., and Nischeta, V. (1969). *Izv. Akad. Nauk. SSSR Neorg. Mat.* 5, 1563.

Conflict of Interest: The authors declare that the research was conducted in the absence of any commercial or financial relationships that could be construed as a potential conflict of interest.

Publisher's Note: All claims expressed in this article are solely those of the authors and do not necessarily represent those of their affiliated organizations, or those of the publisher, the editors and the reviewers. Any product that may be evaluated in this article, or claim that may be made by its manufacturer, is not guaranteed or endorsed by the publisher.